the plant journal

SEB SOCIETY FOR EXPERIMENTAL BIOLOGY

The Plant Journal (2019) doi: 10.1111/tpj.14588

Mutations in the miR396 binding site of the growth-regulating factor gene *VvGRF4* modulate inflorescence architecture in grapevine

Susanne Rossmann[1], Robert Richter[2], Hequan Sun[1], Korbinian Schneeberger[1], Reinhard Töpfer[2], Eva Zyprian[2] and Klaus Theres[1,*]

[1]*Max Planck Institute for Plant Breeding Research, 50931 Cologne, Germany, and*

[2]*Federal Research Centre for Cultivated Plants, Institute for Grapevine Breeding Geilweilerhof, Julius-Kuehn Institute, 76833 Siebeldingen, Germany*

Received 6 February 2019; revised 27 September 2019; accepted 11 October 2019.
*For correspondence (e-mail theres@mpipz.mpg.de).

SUMMARY

Bunch rot caused by *Botrytis cinerea* infections is a notorious problem in grapevine cultivation. To produce high quality fruits, grapevine plants are treated with fungicides, which is cost intensive and harmful to the environment. Conversely, loose cluster bunches show a considerably enhanced physical resilience to bunch diseases. With the aim to identify genetic determinants that modulate the development of bunch architecture, we have compared loose and compact 'Pinot noir' clones. Loose cluster architecture was found to be correlated with increased berry size, elongated rachis and elongated pedicels. Using transcriptome analysis in combination with whole genome sequencing, we have identified a growth-regulating factor gene, *VvGRF4*, upregulated and harbours heterozygous mutations in the loose cluster clones. At late stages of inflorescence development, the mRNA pools of loose cluster clones contain predominantly mRNAs derived from the mutated alleles, which are resistant to miR396 degradation. Expression of the *VvGRF4* gene and its mutated variants in Arabidopsis demonstrates that it promotes pedicel elongation. Taken together, VvGRF4 modulates bunch architecture in grapevine 'Pinot noir' clones. This trait can be introduced into other cultivars using marker-assisted breeding or CRISPR-Cas9 technology. Related growth-regulating factors or other genes of the same pathway may have similar functions.

Keywords: growth-regulating factor (GRF), VvGRF4, *Vitis vinifera* (grapevine), rachis length, pedicel length, Pinot noir, bunch compactness, miR396.

INTRODUCTION

Grapevine (*Vitis vinifera* L. subsp. *vinifera*) is one of the most important fruit crops worldwide with an area of 7.5 million hectares under cultivation, used for wine production, table grapes and raisins (OIV, 2017). *V. vinifera* is susceptible to different diseases and pests such as powdery mildew, downy mildew and *Botrytis*. One of the most serious diseases is bunch rot, caused by *Botrytis cinerea* (*Botryotinia fuckeliana*) with infestation favoured by humid and warm weather conditions during the ripening period (Nair and Allen, 1993; Broome *et al.*, 1995; Vail *et al.*, 1998; Konrad *et al.*, 2003; Deytieux-Belleau *et al.*, 2009; Hed *et al.*, 2009; Molitor *et al.*, 2012) as well as by dense bunch architecture. To produce high quality fruits, grapevine plants are usually treated with fungicides and other protective chemicals (Pertot *et al.*, 2017), which are cost intensive and harmful to the environment. An efficient alternative is breeding and clonal selection of genotypes that develop loose bunches, which show a considerably enhanced physical resilience against *Botrytis* bunch rot (Gabler *et al.*, 2003). In comparison with compact bunches, loose bunch architecture is correlated with a lower level of bunch diseases, for example *Botrytis cinerea* infections (Vail, 1991; Vail *et al.*, 1998; Valdés-Gómez *et al.*, 2008; Hed *et al.*, 2009), which has been explained by reduced humidity in the bunch due to better ventilation and an accelerated drying process (Hed *et al.*, 2010; Molitor *et al.*, 2012). Furthermore, loose bunch architecture promotes uniform berry ripening and positively affects biochemical berry composition (Pieri *et al.*, 2016). Bunch compactness is a complex trait that refers to the arrangement of berries within a bunch and the proportion of free space between them. Bunch architecture is strongly influenced by berry traits, such as number of berries and berry size, as well as by

© 2019 The Authors.
The Plant Journal published by Society for Experimental Biology and John Wiley & Sons Ltd
This is an open access article under the terms of the Creative Commons Attribution-NonCommercial-NoDerivs License, which permits use and distribution in any medium, provided the original work is properly cited, the use is non-commercial and no modifications or adaptations are made.

stalk characteristics, like rachis length and pedicel length (Tello and Ibáñez, 2017; Richter *et al.*, 2019). These traits, varying widely between cultivars, are regulated by genetic factors, but can also be modulated by environmental parameters and management strategies. In a comparison between two compact ('Chardonnay' and 'Riesling') and two loose cluster ('Exotic' and 'Sultana') cultivars, inflorescence length was identified as the major trait affecting the phenotypic difference (Shavrukov *et al.*, 2004), whereas in the cultivar 'Albariño', berry size was identified as the variable exerting the major influence on *Botrytis* resilience (Alonso-Villaverde *et al.*, 2008). Agronomic strategies, such as gibberellic acid (GA) application, can enhance pedicel length and thickness in 'Sultana' (Sarooshi, 1977) or reduce berry number, when applied at flowering time to table grapes and wine grapes (Lynn and Jensen, 1966; Christodoulou *et al.*, 1968; Mosesian and Nelson, 1968).

The development of grapevine inflorescences, called panicles (Pratt, 1971), extends over two consecutive growing periods. In the first year, inflorescences develop within a latent bud, including the formation of inflorescence meristems and the differentiation of primary branches. After a dormancy period during winter, buds burst, inflorescences rapidly elongate, secondary and tertiary branches differentiate and floral meristems initiate (Carmona *et al.*, 2002). The number of flowers per inflorescence together with the rate of pollination and the development of flowers into berries (fruit set rate) determines the final number of berries in a bunch. After fruit set, individual berries start to grow reaching at ripening their final size, which can vary considerably between cultivars (Houel *et al.*, 2013), depending on genetic determinants, the nutritional status and the viticultural management strategies applied (Tello and Ibáñez, 2017).

Among the genetic determinants that control growth and development of inflorescences in plants, transcriptional regulators play a prominent role. Growth-regulating factors (GRFs), which are mainly expressed in young actively growing tissues, form a small plant-specific subgroup of transcriptional regulators (reviews: Kim and Tsukaya, 2015; Omidbakhshfard *et al.*, 2015). In their N-terminal region, GRFs contain the characteristic QLQ and WRC sequence motifs, mediating protein–protein interactions and DNA binding, respectively (van der Knaap *et al.*, 2000, Kim *et al.*, 2003, Zhang *et al.*, 2008, Kuijt *et al.*, 2014). The C-terminal region of GRF proteins is highly variable and mediates transactivation activity in several members of the gene family (Kim and Kende, 2004; Liu *et al.*, 2014a). As shown by yeast-two-hybrid interaction and bimolecular fluorescence complementation studies, GRFs form complexes with GRF interacting factors (GIFs), which belong to a small group of transcriptional co-activators, to exert their function (Kim and Kende, 2004; Horiguchi *et al.*, 2005). Transcript accumulation of the majority of GRFs is regulated by microRNA396 (miR396), which shows almost perfect sequence complementarity with the *GRF* mRNA sequence that encodes the WRC domain (Liu *et al.*, 2009; Rodriguez *et al.*, 2010). The different GRFs have specific biological functions, but act also redundantly, regulating many processes in plant growth and development (Omidbakhshfard *et al.*, 2015). Among other processes, GRFs modulate leaf and cotyledon size (Kim *et al.*, 2003; Liu *et al.*, 2009; Rodriguez *et al.*, 2010; Wang *et al.*, 2011; Debernardi *et al.*, 2014), seed (Liu *et al.*, 2012), flower (Baucher *et al.*, 2013; Liang *et al.*, 2014; Pajoro *et al.*, 2014; Liu *et al.*, 2014a) and root development (Hewezi *et al.*, 2012; Bazin *et al.*, 2013). Furthermore, recent studies uncovered functions of GRFs in leaf senescence (Debernardi *et al.*, 2014) and in the coordination of plant growth with abiotic and biotic stress responses (Liu *et al.*, 2014b). Several examples show that GRF upregulation correlates with an increase in organ size, due to an increase in cell size (Kim *et al.*, 2003) or an enhancement of cell proliferation (Debernardi *et al.*, 2014; Wang *et al.,* 2014). However, Arabidopsis GRF9 (Omidbakhshfard *et al.*, 2018) and the maize GRF10 protein (Wu *et al.*, 2014) restrict cell proliferation in the developing leaves resulting in reduced leaf size, which indicates that modulation of GRF activity can have opposite consequences for plant development. GRF-homologous sequences have been identified in all land plant genomes sequenced to date and many GRFs have been functionally characterized in Arabidopsis, rice, maize and in many other plant species (Omidbakhshfard *et al.*, 2015).

In this study, we have compared bunch architecture of loose and compact 'Pinot noir' (PN) clones. In contrast with the compact clones Frank Charisma (FCh) and Frank Classic (FCl), the loose cluster clones WE M171 (M171) and 1-86 Gm (1-86) developed elongated pedicels due to an enhanced cell division rate or an extended window of cell proliferation. RNA-seq analysis revealed that transcript abundance of the GRF *VvGRF4* is upregulated in these loose cluster clones, because cleavage of *VvGRF4* mRNA by miR396 is disrupted due to mutations in the miR396 binding site. *VvGRF4* overexpression in Arabidopsis accelerated pedicel growth and this effect is enhanced, if the miR396 binding site of *VvGRF4* is mutated.

RESULTS

Genetic and phenotypic diversity in cluster architecture among 'Pinot noir' clones

'Pinot noir' (PN) clones show a lot of variation in inflorescence architecture. To study the differences between loose and compact cluster clones, we took advantage of the clonal diversity existing in PN. Four different PN cluster types can be distinguished: compact, loose, upright growing and mixed berry size (Porten, 2001). The loose cluster PN clones are represented by the so-called Mariafeld (M)-types

© 2019 The Authors.

from Wädenswil (Switzerland), selected since 1965 (Huber, 1965) and the Geisenheim (Gm)-types from Geisenheim (Germany), which have been selected since 1981 (Schmid *et al.*, 2009). In this study, we focused on the M-type loosely clustered clone (LCC) WE M171 (M171) and the Gm-type clone 1-86 Gm (1-86), which were compared with the compact cluster clones (CCCs) Frank Charisma (FCh) and Frank Classic (FCl) (Figure 1a–d).

As little information is known about the genetic diversity of these clones, we first determined the genetic relatedness based on 87 single nucleotide polymorphisms (SNPs) identified by genomic DNA sequencing. FCh and FCl are most similar (Figure 1e), which is in line with the fact that these clones were initially selected from the same progenitor (Frank, 2006). The two LCCs grouped separately from the CCCs with 1-86 being most distantly related (Figure 1e). These data indicate that the two LCCs are not only distinct from the CCCs, but also genetically diverse among each other, most likely because they were derived in different clonal selection processes.

Variability of cluster architecture can be explained by parameters, like rachis length, berry number, berry volume etc. To better understand loose cluster architecture, we have monitored several aspects of cluster development in the LCCs M171 and 1-86 in comparison with CCCs over two consecutive years. For both LCCs, the same three parameters of cluster architecture turned out to be significantly different from CCC clones in almost all pairwise comparisons: Rachis length, pedicel length and berry size were increased in LCCs (Figure 1f–i and Supporting Information Figure S1). Whereas the increase in rachis length and pedicel length can be easily correlated with the loose cluster phenotype, the increase in berry size was counterintuitive. Although the two types of LCCs are genetically diverse, the above experiments clearly demonstrated that a common set of determinants, including rachis length, pedicel length and berry size, is sufficient to describe the main differences in their cluster phenotype.

Pedicels of loose cluster clones show an enhanced number of cells

Elongated pedicels can be a result either of cell elongation or of an increase in cell number, due to more cell divisions. To distinguish between these alternative hypotheses, Scanning electron microscopy (SEM) micrographs of pedicel epidermal cells were taken and cell width along the longitudinal axis was measured (Figure 2a,d–g). However, no significant difference in cell size was detected, when either M171 or 1-86 were compared with the CCCs (Figure 2b), suggesting that not an increase in cell width but an increase in cell number is responsible for the elongated pedicel phenotype. To test this hypothesis, cell number was determined in the pedicel epidermis, where cells are arranged in rows (Figure 2d–g). To determine the total number of cells in a row, pedicel length was divided by the average cell width. LCCs had significantly more cells than CCCs (Figure 2c), indicating an enhanced rate of cell divisions or an extended period of cell proliferation during pedicel development in both LCCs.

Transcript abundance of a mutated *VvGRF4* gene is upregulated in loose cluster clones

To identify genes that promote loose cluster architecture in M171 and 1-86, comparative transcriptome analyses of inflorescences of three different developmental stages were performed. At the end of the first growing season, a compressed shoot has developed within a latent bud, including a shoot apical meristem, young leaves and two premature inflorescences (Figure 3a–c) (Carmona *et al.*, 2002). Stage 1 samples contained inflorescences that were dissected from such latent buds. Stage 2 inflorescences were collected from buds at the time of bud burst (BBCH9) (Lorenz *et al.*, 1995) (Figure 3d–f). The third sample (stage 3), which was harvested just before flower opening at BBCH57 stage (Lorenz *et al.*, 1995) (Figure 3g,h), contained mainly rachis tissue without flowers. High-quality reads were mapped to the grapevine genome (Table S1) and expression values (RPKM, reads per kilo base per million mapped reads) were calculated. Each LCC was compared separately with FCh and FCl. LCC genes were considered to be differentially expressed, if their RPKM value was significantly different from that of the corresponding gene in at least one CCC ($\geq$1.5-fold, P-value $\leq$ 0.05). In total, 582 differentially expressed genes (DEGs) could be identified in M171 (Figure 3i and Data S1) and 1308 in 1-86 (Figure 3j and Data S2), with some genes (20 in M171 and 94 in 1-86) being differentially expressed at least at two stages (Figure 3i,j). Overall, 383 DEGs were shared between M171 and 1-86 (Figure 3k).

As a second unrelated approach, we have used whole genome sequencing to detect unique variants in LCC genomes, such as SNPs as well as insertions and deletions in coding sequences (CDS), introns, untranslated regions (UTRs) and in 3 kb upstream and downstream regions. In total, 690 genes in M171 and 1078 genes in 1-86 carried at least one sequence alteration in comparison with both CCCs (Data S3). These lists were compared with the respective lists of DEGs. In M171, only 12 out of the 582 DEGs contained a unique mutation (Figure 3l). Two of these 12 genes carried an SNP within the coding sequence that caused an amino acid exchange (Data S4). In 1-86, 36 out of 1308 DEGs carried a DNA sequence alteration (Figure 3m), of which one non-synonymous and two synonymous mutations were localized within the coding region (Data S4). Only one gene, VIT_16s0039g01450, was differentially expressed in both LCCs and carried unique mutations in both LCCs (Figure 3n and Data S4). VIT_16s0039g01450 encodes Growth-Regulating-Factor 4

© 2019 The Authors.

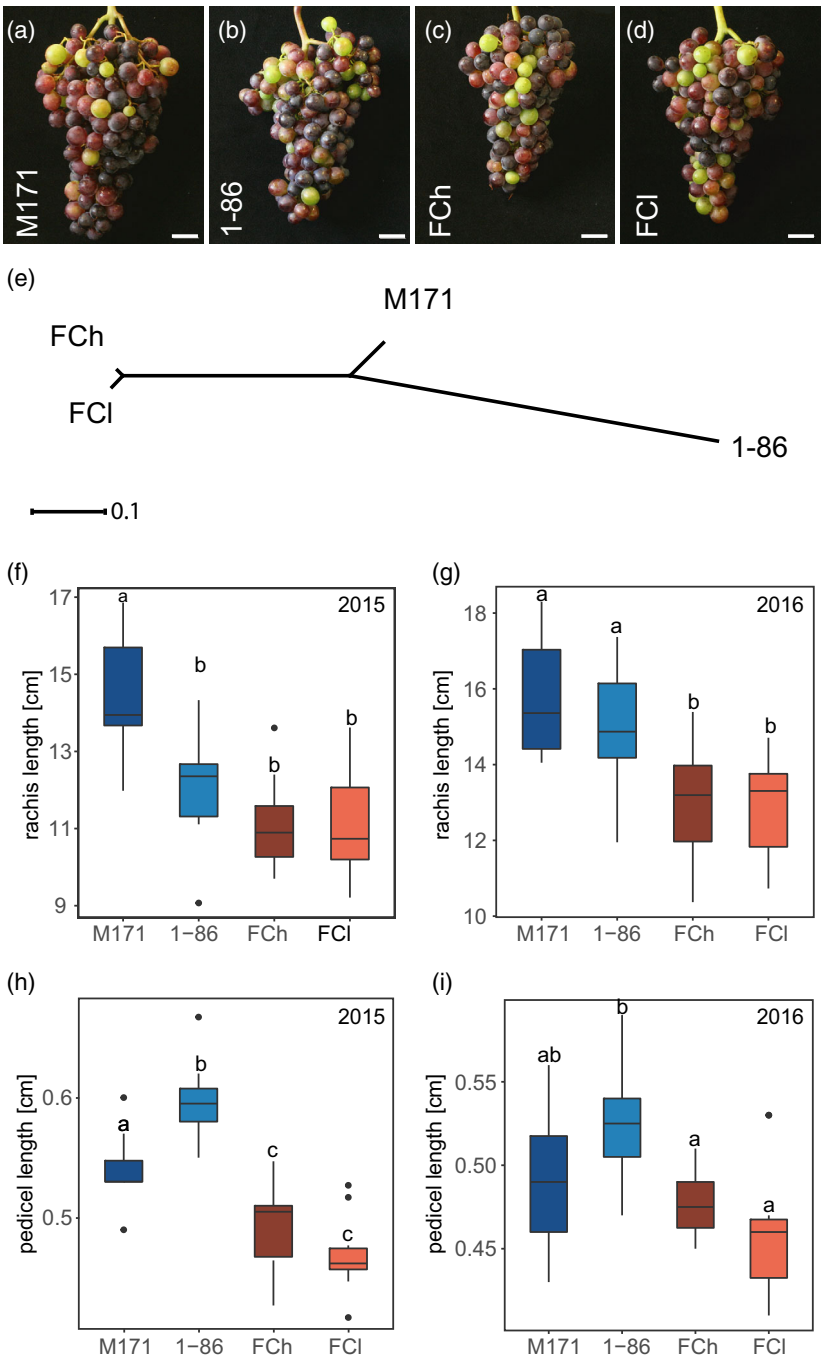

Figure 1. Loose cluster architecture in We M171 and 1-86 Gm clones is caused by an increase in rachis and pedicel length.
(a–d) Photographs showing the bunch phenotype of the loose cluster clones We M171 (M171) (a) and 1-86 Gm (1-86) (b), and the compact cluster clones Frank Charisma (FCh) (c) and Frank Classic (FCl) (d). Scale bars: 2 cm. (e) Phylogenetic tree based on 87 SNPs. (f–i) Box plots of rachis length (f, g; $n = 10$) and pedicel length (h, i, $n = 10$ of 10 bunches), measured in 2015 (f, h) and 2016 (g, i), respectively. Black dots represent outliers. Different letters indicate significantly divergent mean values (Tukey's honest significant difference (HSD), $P < 0.05$).

(VvGRF4) belonging to a small family of plant-specific transcription factors (Omidbakhshfard *et al.*, 2015). The mutations in the *VvGRF4* genes of M171 and 1-86 are located in the second exon of the gene, separated only by a single base pair, and both are in heterozygous condition (Figure 4a). The SNP in 1-86 (327TA) is synonymous, whereas the 329C to T transition in M171 causes an amino acid exchange from serine to leucine (Figure 4a) in the highly conserved WRC domain (Figure S2), suggested to be involved in DNA binding. The two mutant alleles were named *VvGRF4-m1* (M171) and *VvGRF4-m2* (1-86).

VvGRF4-m1 and *VvGRF4-m2* mRNAs are resistant to miR396

mRNA abundance of most GRFs is regulated by microRNA miR396 binding to a conserved recognition site within the WRC domain (Omidbakhshfard *et al.*, 2015). Also *VvGRF4* contains the miR396 complementary sequence and the

© 2019 The Authors.

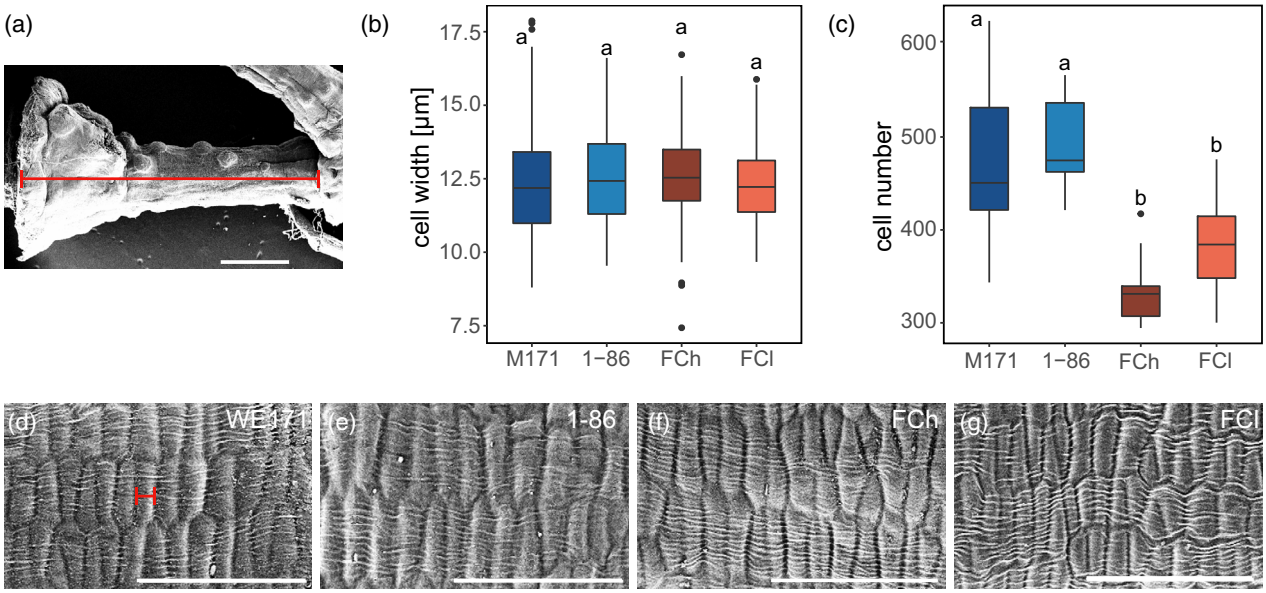

Figure 2. Pedicels of loose cluster clones show a higher number of cells.
(a) Scanning electron micrograph (SEM) picture of an FCl pedicel. Red bar indicates pedicel length. (b) Width of pedicel cells (n = 100/pedicel, at least seven pedicels were measured) did not show a significant difference between loose cluster clones (LCCs) and compact cluster clones (CCCs). (c) LCCs contain a significantly higher number of cells in their pedicels (calculated per row as pedicel length) than CCCs. (d–g) SEM images of epidermis cells obtained from M171 (d), 1-86 (e), FCh (f) and FCl (g) pedicels. Images were taken from similar positions in the middle part of the pedicel and are oriented as in (a). In (b) and (c), different letters indicate that mean values are significantly different from each other, whereas the same letters indicate no significant difference (Tukey's HSD, $P < 0.05$). Black dots represent outliers. Red bar in (d) indicates the width of a cell in longitudinal orientation, as used for measurements in (c). Scale bars: 1 mm (a), 100 µm (d–g).

identified SNPs in *VvGRF4-m1* and *VvGRF4-m2* are both located in the putative miR396 binding sequence (Figure 4b, Figure S3). The RLM-Race (5′RNA ligase-mediated rapid amplification of cDNA ends) technique was applied to map the VvmiR396-cleavage site within *VvGRF4* mRNA of the compact cluster clone FCh. Sequence analysis revealed that the 5 ends of cleaved mRNA fragments in 12 out of 14 randomly selected clones mapped to the same position within the VvmiR396 recognition sequence (Figure 4b). These results demonstrate that miR396 cleaves *VvGRF4* mRNA *in vivo*, corroborating the recent findings by Pantaleo *et al.* (2016).

VvGRF4 mRNA levels of CCCs were highest at stage 1 with RPKM values around 90, dropping to around 10 at stage 3 in both compact cluster clones, with intermediate expression levels at stage 2 (Figure 4c). The mRNA level of *VvGRF4* negatively correlates with abundance of pri-miR396 transcripts, which were mainly derived from the genes miR396a and miR396b at stage 2 and stage 3, when highest expression levels were reached (Figure 4d,e). miR396c and miR396d were expressed at very low levels. qRT-PCR experiments confirmed the negative correlation between transcript levels of mature miR396 and *VvGRF4* at stage 2 and 3 (Figure 4f,g).

At stage 2 and stage 3, *VvGRF4* mRNA was kept at high levels in LCC, which are heterozygous for the mutated *VvGRF4* alleles, whereas CCCs showed a maximum reduction of 2.1 and 3.9 in RNA-seq data and qRT-PCR analysis, respectively (Figure 4c,f). Is this variation in *VvGRF4* mRNA abundance a consequence of differential cleavage of the different transcripts by miR396? The predicted minimum free energy values for miR396 binding increased from −33.7 for *VvGRF4* (CCC) to −31.5 for *VvGRF4-m1* (M171) and to −30.2 kcal mol^{-1} for *VvGRF4-m2* (1-86) (Figure 4b). This suggests that cleavage of the mutated mRNAs by miR396 may be disrupted, which could explain the elevated *VvGRF4* transcript levels in LCCs at stage 2 and 3, when miR396 expression is upregulated. To test this hypothesis, we sequenced RT-PCR products of M171 and 1-86 transcripts. At stage 2, when miR396 is moderately expressed, mutated alleles (*VvGRF4-m1* and *VvGRF4-m2*) and the compact cluster allele (*VvGRF4*) are equally represented, as expected for a heterozygous situation (Figure 4h,i). Only at stage 3, the mRNA pools are dominated by the *VvGRF4-m1* and *VvGRF4-m2* forms (Figure 4h,i). Sequencing of randomly selected RT-PCR clones verified that 23/24 (M171) and 20/23 (1-86) clones represented the mutant alleles (Figure 4h,i). Similar results were obtained by RNA-seq analysis detecting around 50% mutated mRNAs at stage 2, whereas at stage 3 83% (M171) and 77% (1-86) mutated transcripts were found (Table S2). These results suggest that the cleavage of *VvGRF4-m1* and *VvGRF4-m2* transcripts by VvmiR396 is disrupted, preventing a downregulation of the respective mRNA pools.

© 2019 The Authors.

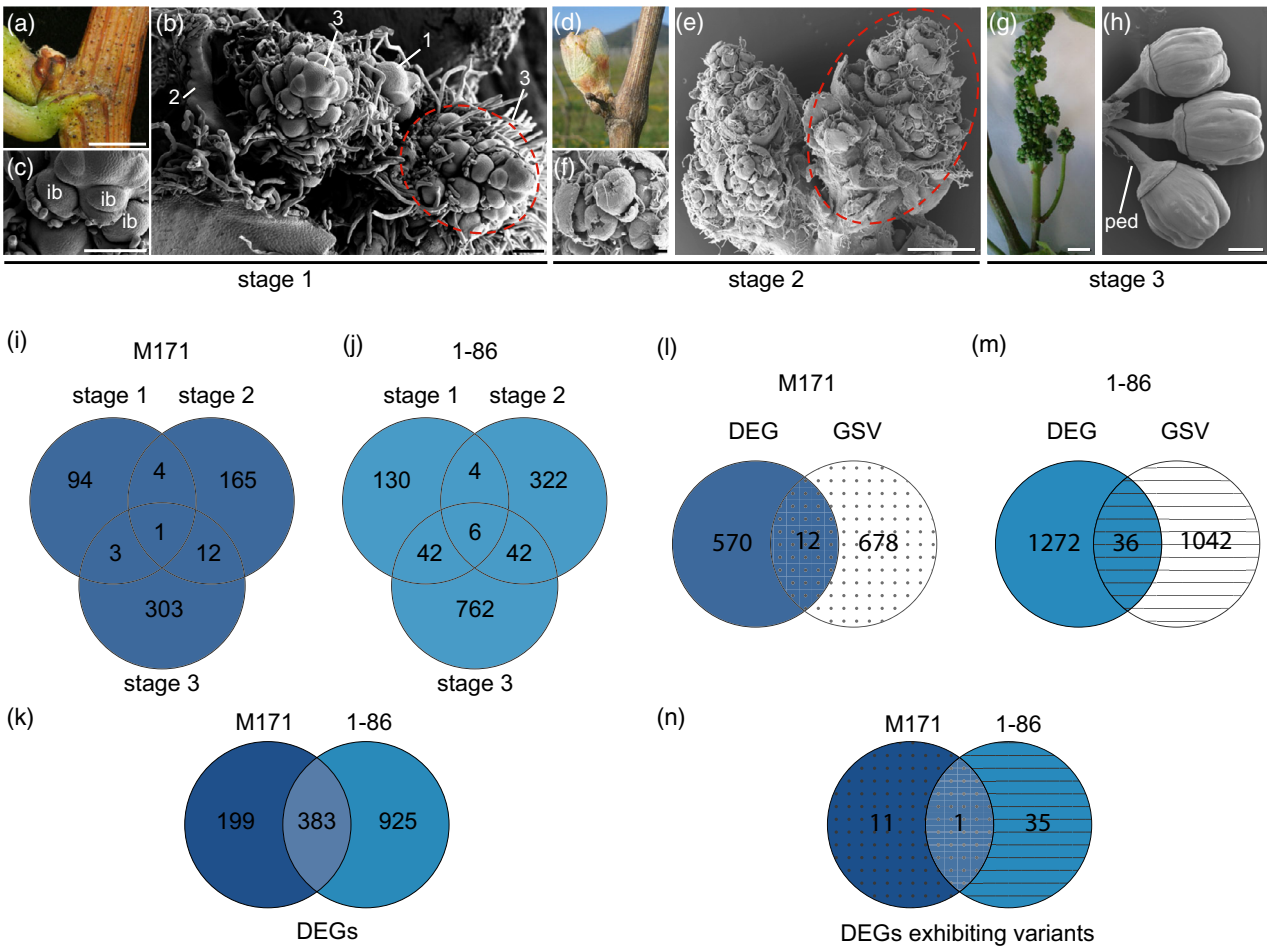

Figure 3. Identification of gene variants differentially expressed in loose cluster clones.
(a–h) Inflorescence development in *Vitis vinifera* (grapevine), 'Pinot noir', at three different stages. (a) Latent bud (stage 1) in a leaf axil before bud dormancy. (b) SEM image of a compressed shoot within a stage 1 bud, including shoot apical meristem (1), leaves (2) and immature inflorescences (3). Dashed line marks the tissue used for RNA-seq analysis (stage 1). (c) Close up view of (b), showing inflorescence branch meristems (ib). (d) A BBCH9 (stage 2) bud at bud burst. (e, f) Developing inflorescences with flowers; (f) shows close up of (e) in a stage 2 bud. Dashed line marks the tissue used for RNA-seq analysis (stage 2). (g) Grapevine inflorescence/cluster of BBCH57 stage (stage 3) just before flower opening. (h) Detached floral buds characterized by elongated pedicels (ped) at stage 3. Rachis tissue without flowers was used for RNA-seq analysis. (i, j) Venn diagrams showing number of differentially expressed genes (DEGs) (1.5-fold change, *P*-value ≤0.05) in M171 (i) and 1-86 (j) compared with compact cluster clones FCl and FCh. (k) DEGs found in M171 and 1-86. (l, m) Venn diagrams showing the overlap between DEGs and genes exhibiting sequence variations (GSVs) in M171 (l) and 1-86 (m). (n) One common DEG contains mutations in both loose cluster clones. Scale bars: 100 μm (b, c, f), 1 mm (e, h), 1 cm (a, g).

Mutations in the miR396 binding site of *VvGRF4* seem to be specific for 'Pinot noir' LCCs

As previously mentioned, M171 belongs to the M-type and 1-86 to the Gm-type of 'Pinot noir' LCCs. To check whether the miR396 binding site is mutated in other 'Pinot noir' LCCs, we sequenced the miR396 binding site of *VvGRF4* of further M-type and Gm-type loose cluster clones ($n = 6$). Sequencing results revealed that all M-type clones carried the *VvGRF4-m171-1* allele, whereas the *VvGRF4-1-86-1* allele was specific for all Gm-type clones, in each cases in heterozygous condition (Table S3). This positive correlation indicates that these mutations are causal for the loose cluster bunch architecture, supported by the fact that none of the tested CCCs ($n = 6$) carried any mutation in the miR396 binding site (Table S3).

To test whether the same or additional *VvGRF4* alleles had been selected by breeders in other varieties, we sequenced the miR396 binding site of additional cultivars and clones with loose cluster architecture, including table grapes and reference varieties (Table S3). In 13 varieties, we could not identify any mutation in the miR396 binding sequence (Table S3), which indicates that the *VvGRF4-m1* and *VvGRF4-m2* alleles are specific for 'Pinot noir' LCCs.

VvGRF4 orthologues in tomato modulate pedicel length

The GRF transcription factor family includes 10 proteins in grapevine (http://www.gramene.org, release 54, May 2018),

© 2019 The Authors.

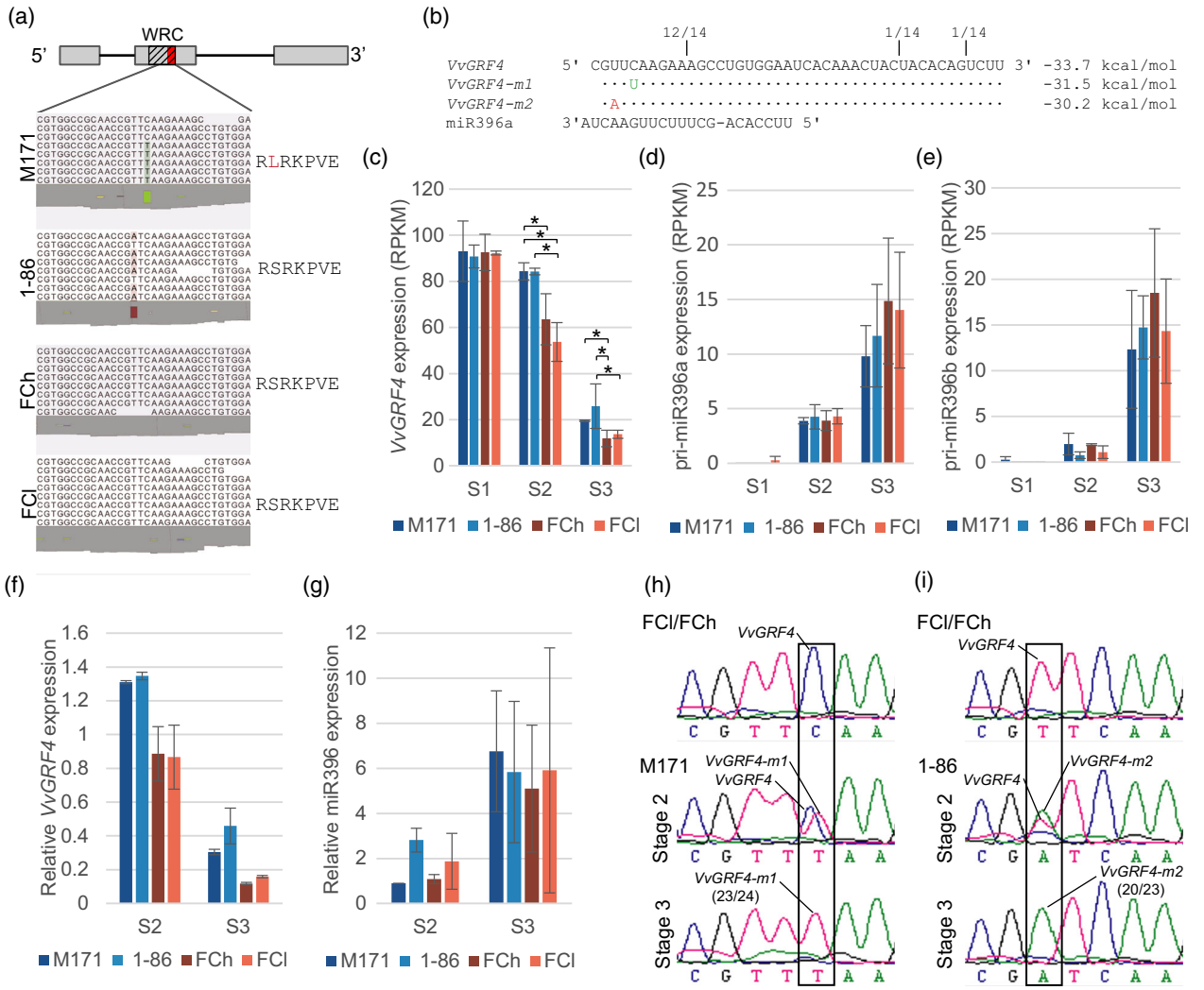

Figure 4. Mutated *VvGRF4* transcripts are resistant to downregulation by miR396.
(a) Mapping profiles of RNA-seq reads. Both loose cluster clones M171 and 1-86 contain a unique, heterozygous SNP in the VvGRF4 miR396 binding site (red), located within the WRC domain (striped box). The M171 SNP leads to an amino acid exchange. (b) Transcript degradation fragments of FCh *VvGRF4* mRNA as mapped by RLM-RACE. Numbers on top give the ratio of clones with 5′-ends mapping at a specific position relative to the total number of sequenced clones. Numbers on the right indicate the predicted minimum free energy hybridization values between miR396 and *VvGRF4* (FCh), *VvGRF4-m1* (M171) and *VvGRF4-m2* (1-86), respectively, as determined by RNAhybrid (Rehmsmeier *et al.*, 2004). (c–e) Expression of *VvGRF4* (c), pri-miR396a (d) and pri-miR396b (e) at stage 1 (S1), stage 2 (S2) and stage 3 (S3), as quantified by RNA-seq analysis. Values are means of two (S1) or three (S2, S3) biological replicates, including standard deviation (SD). RPKM is reads per kilo base per million mapped reads. Asterisks indicate significant differences at a *P*-value of 0.05. (f, g) Quantification of *VvGRF4* (f) and mature miR396 (g) transcripts by qRT-PCR at S2 and S3. *VvGRF4* values were normalized with *GAPDH*, miR396 with U6 and 5.8S. Values represent means of two biological replicates harvested in 2015 including SD. (h, i) Chromatograms of sequenced RT-PCR (reverse transcription PCR) products amplified with primers flanking the cleavage site in *VvGRF4* using cDNA of M171 (h) and 1-86 (i) from S2 and S3 in comparison to FCl/FCh. Numbers above the chromatograms at S3 give the ratio of mutant alleles [*VvGRF4-m1* (h) and *VvGRF4-m2* (i)] relative to the total number of sequenced RT-PCR clones.

nine in *Arabidopsis thaliana* (Arabidopsis) (Kim *et al.*, 2003), 13 in *Solanum lycopersicum* (tomato) (Cao *et al.*, 2016) and 12 in *Oryza sativa* (rice) (Choi *et al.*, 2004). Phylogenetic analysis of amino acid sequences from these four species grouped VvGRF4 with three tomato proteins (SlGRF1, SlGRF2 and SlGRF3) and three rice proteins (OsGRF3, OsGRF4 and OsGRF5), but not with any Arabidopsis protein (Figure S4), indicating the lack of a *VvGRF4* orthologue in Arabidopsis.

In tomato, a blockage of miR396 binding using a short tandem target mimic approach led to a strong upregulation of *SlGRFs* expression, including the three *VvGRF4* orthologues *SlGRF1*, *SlGRF2* and *SlGRF3* (Cao *et al.*, 2016). Previously, it was shown that fruit size was increased in these transgenic plants (Cao *et al.*, 2016). Interestingly, pedicel length is also significantly increased in these transgenic plants in comparison to the wild-type (Figure 5a; Cao *et al.*, 2016). However, neither in wild-type nor in

© 2019 The Authors.
The Plant Journal published by Society for Experimental Biology and John Wiley & Sons Ltd,

transgenic plants we observed a correlation between fruit width and pedicel length (Figure 5b). Comparing fruits of similar width, the corresponding pedicels of transgenic plants were longer than those of the wild-type, suggesting a strong impact of SlGRFs on pedicel development independent of fruit size (Figure 5b). Phenotypically, the elongated pedicels caused a more open truss architecture (Figure 5c–e), resembling the loose cluster architecture found in grapevine.

Overexpression of *VvGRF4* in Arabidopsis causes an increase in pedicel length

To study the biological role of VvGRF4 and to test whether the mutations detected in M171 and 1-86 are causal for the elongated pedicel phenotype, we designed three different constructs, overexpressing the compact cluster *VvGRF4* allele (OEVvGRF4) and the mutated alleles of M171 (OEVvGRF4-m1) and 1-86 (OEVvGRF4-m2) (Figure 6a). As it is not feasible to monitor the consequences of *VvGRF4* overexpression in transgenic grapevine plants, because it would take several years before such plants would develop inflorescences, we introduced the overexpression constructs into Arabidopsis accession Col-0. Sequence comparisons revealed a very high conservation of miR396 binding sites between Arabidopsis and grapevine GRFs (Figure S3), which led us to hypothesize that the Arabidopsis miR396 machinery is capable of downregulating the *VvGRF4* mRNA, but not the resistant versions *VvGRF4-m1* and *VvGRF4-m2*. We obtained 19 independent OEVvGRF4, 12 OEVvGRF4-m1 and 35 OEVvGRF4-m2 T0 lines. Many of these lines did not produce seeds. After determination of copy number by qPCR, we selected several single copy lines (four to six lines per construct) for further analysis. In the Arabidopsis overexpression lines OEVvGRF4 #2 and #3, RLM-Race experiments revealed the same miR396-cleavage site within *VvGRF4* mRNA as monitored in grapevine (Figure S5). These results demonstrate that VvGRF4 was cleaved by miR396 in Arabidopsis. *VvGRF4* mRNA levels were monitored by qPCR using primers specific for *VvGRF4*, not binding to any *AtGRF* sequence. Except for two lines, which did not express *VvGRF4* (OEVvGRF4-m1 #1 and OEVvGRF4-m2 #3), transcript levels were higher in transgenic plants expressing the mutated versions compared with OEVvGRF4 (Figure 6b), supporting our hypothesis that the mutated *VvGRF4* mRNAs cannot be cut by Arabidopsis miR396. Those lines showing elevated *VvGRF4* transcript levels were used for further analyses.

Homozygous and heterozygous plants of segregating T2 populations were compared with null segregants, lacking the transgene. Independently of the introduced transgene, most of the transgenic plants produced significantly more rosette leaves and bolted later than the corresponding null segregants (Figure S6a,b). Homozygous plants, overexpressing the mutated versions of *VvGRF4*, often terminated main inflorescence development very early, whereas side

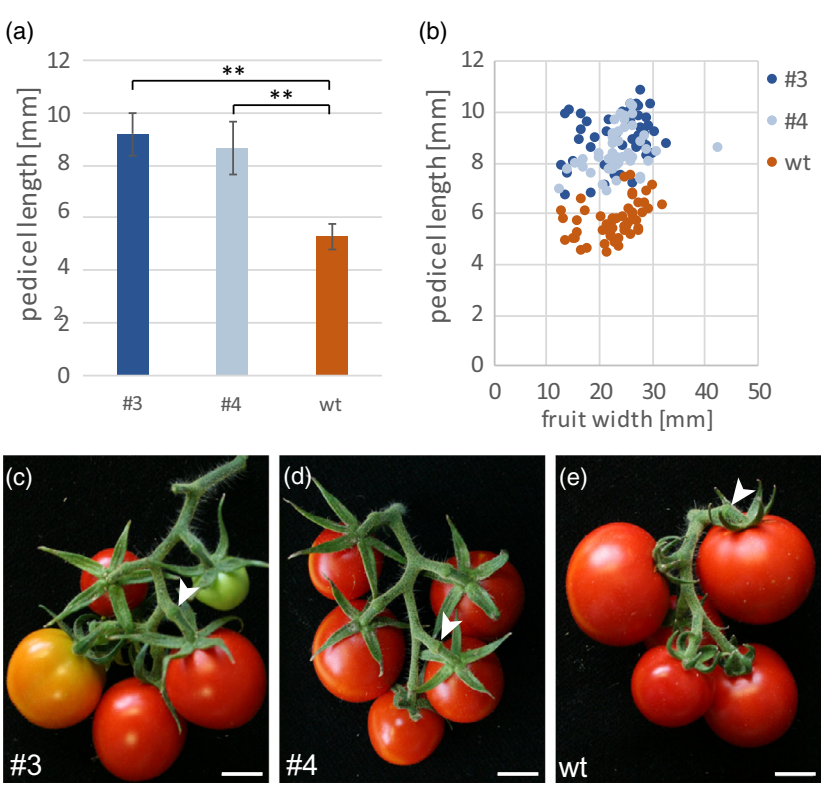

Figure 5. Upregulation of *GRFs* in tomato conditions longer pedicels.
(a) The transgenic tomato lines #3 and #4, in which *SlGRF* expression was upregulated (Cao *et al.*, 2016), developed longer pedicels compared with Micro-Tom wild-type plants (wild-type (wt); $n = 50$ per genotype). Asterisks indicate significant differences (one way ANOVA, post hoc Tukey test; $P < 0.01$). (b) Pedicel length does not correlate with fruit width, neither in wild-type ($R^2 = 0.18$) nor in the transgenic lines (#3, $R^2 = 0.07$; #4, $R^2 = 0.09$). Data points show the relationship between fruit width and pedicel length of individual fruits ($n = 50$ per genotype). (c–e) In contrast with wild-type (e), transgenic lines #3 and #4 (c, d), developed fruit trusses showing a loose architecture. Arrowheads point to abscission zone. Scale bars, 1 cm.

© 2019 The Authors.

shoots developed normally (Figure S7a). For that reason, main inflorescence length, a trait comparable to rachis length in grapevine, which was increased in LCCs (Figure 1) was compared between heterozygous plants and null segregants. Transgenic plants carrying the mutated *VvGRF* transgenes (*OEVvGRF4-m1* or *OEVvGRF4-m2*) developed significantly longer main inflorescences than null segregants, whereas main inflorescence length was not increased in transgenic plants carrying the FCh version (*OEVvGRF4*) (Figure 6c).

In Arabidopsis, pedicel elongation strongly depends on progression of flower and silique development (Yamaguchi and Komeda, 2013). In contrast with null segregants, we observed that all lines, overexpressing the mutated versions of *VvGRF4* exhibited strong abnormalities in silique development (Figure S7b–d,f). Therefore, only pedicels of normally developed siliques were measured and compared between heterozygous plants and null segregants (Figure S7e,f). Transgenic plants of all three OEVvGRF4-m1 lines and three out of five OEVvGRF4-m2 lines showed a significant increase in pedicel length compared with the respective control plants (Figure 6d). Even two out of four OEVvGRF4 transgenic lines developed significantly longer pedicels (Figure 6d). However, on average the difference in pedicel length between OEVvGRF4 and control plants was only 0.62 ± 0.55 mm, whereas the difference between OEVvGRF4-m1 and control plants was 1.98 ± 0.14 mm (Figure 6e). These data suggest that VvGRF4 accelerates pedicel growth and that this effect is enhanced, if the miR396 binding site of *VvGRF4* is mutated.

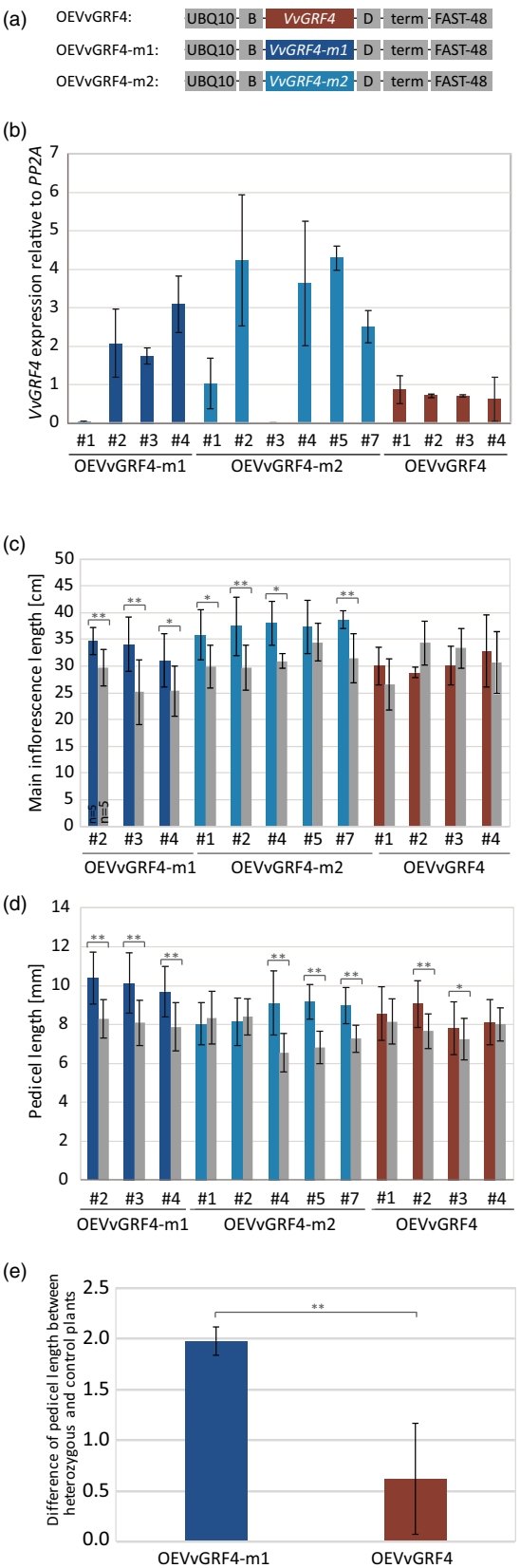

Figure 6. Pedicel length is significantly increased in Arabidopsis plants overexpressing the mutated form VvGRF4-m1.
(a) Schematic representation of DNA constructs, in which the UBIQUITIN10 promoter (UBQ10) is driving expression of *VvGRF4* and its mutated derivatives *VvGRF4-m1* and *VvGRF4-m2*. Two dummy sequences (see Experimental procedures) were used instead of an N-tag (=B) and a C-tag (=D). term stands for UBQ10 terminator. FAST (fluorescence-accumulating seed technology) cassette (Shimada *et al.*, 2010) was used to identify seeds containing the construct. Blue colour refers to the LCCs M171 and Gm1-86 and brown colour to the CCC FCh. (b) Comparison of *VvGRF4* mRNA accumulation in closed flower buds of OEVvGRF4-m1, OEVvGRF4-m2 and OEVvGRF4 single copy lines. For each replicate, tissue was harvested from two plants harbouring the transgene in heterozygous condition. Transcript levels were normalized using the Arabidopsis gene PP2A as reference. Data are the mean of two biological replicates. (c) Main inflorescence length of heterozygotes (colour filled) in comparison to null segregants (grey filled) from segregating T2 populations of different OEVvGRF4–m1, OEVvGRF4-m2 and OEVvGRF4 lines (n = 3 to 15). (d) Pedicel length of comparable sets of siliques of the main inflorescence in heterozygotes (coloured) versus null segregant plants (grey) of segregating T2 populations in different OEVvGRF4-m1, OEVvGRF4-m2 and OEVvGRF4 lines (n = 5, of at least seven plants). (e) Comparison of the mean of differences observed between heterozygous OEVvGRF4-m1 plants (shown in (d)) and null segregants with the mean of differences in pedicel length observed between heterozygous OEVGRF4 plants and null segregants. Error bars in (b–d) represent SD of the mean. Asterisks in (c) and (d) indicate significant differences (one-way ANOVA, post hoc Tukey test; *P < 0.05, **P < 0.01).

© 2019 The Authors.

DISCUSSION

VvGRF4 regulates bunch compactness in 'Pinot noir'

We have studied the phenotypic and genetic differences between two compact and two loose cluster grapevine clones derived by independent clonal selection from the variety 'Pinot noir'. Our phylogenetic analysis revealed that the two LCCs are genetically quite diverse from each other, confirming the previous classification into M-type and Gm-type clones (Huber, 1965; Schmid *et al.*, 2009). We applied RNA-seq and whole genome DNA-seq analysis to identify candidate genes that are associated with loose cluster architecture. Neither the RNA-seq approach, nor the gDNA-seq approach was sufficient on its own to reduce the number of candidate genes effectively. However, in combination, the two approaches identified a few genes, harbouring mutations in their coding region or in their regulatory sequences, which might explain the observed phenotypic differences between loose and CCCs. Surprisingly, one gene, *VvGRF4*, was differentially expressed in both LCCs and carried different mutations in the two clones, both localized in the miR396 recognition sequence. *VvGRF4* encodes a transcriptional regulator, expressed in young growing tissues, such as seedlings, tendrils and buds (Fasoli *et al.*, 2012). At stage 3 of inflorescence development, when *VvGRF4* expression is high in LCCs compared with CCCs, the mRNA pools of LCCs contain predominantly mRNAs derived from the mutated alleles, which are resistant to miR396 degradation.

Overexpression of the mutated alleles in Arabidopsis resulted in longer inflorescences and pedicels. In rice, a 2 bp substitution in the miR396 binding site of *OsGRF4,* one of the *VvGRF4* orthologues, also leads to an upregulation of transcript abundance and conditions longer panicles (Che *et al.*, 2015; Duan *et al.*, 2015). Sequence comparisons revealed that the mutation in the M171 gene (*VvGRF4-m171-1* allele) co-localizes with one of the base substitutions identified in *OsGRF4* (Figure S3), strongly supporting the view that *GRFs* harbouring mutated miR396 binding sites condition mis-regulation of mRNA levels and are ultimately associated with similar phenotypes, such as enlarged rachis and panicles in grapevine and rice, respectively.

Enhanced number of cells in pedicels leads to loose cluster architecture

Grapevine cluster architecture is a rather complex trait, which can be influenced by many different factors. Tello *et al.* (2015) analyzed 125 grapevine accessions and identified total berry number and length of first ramification as the most important factors influencing bunch compactness. In our study, berry volume, rachis length and pedicel length, turned out to be significantly increased in both M171 and 1-86 in comparison with the CCCs. This can be explained by the fact that in both clones a mis-regulation of the same gene (*VvGRF4*) caused the alteration in phenotype. The increase in rachis length is a characteristic that was also found in many other grapevine cultivars to be responsible for loose cluster architecture (Shavrukov *et al.*, 2004; Tello *et al.*, 2015), however, genes regulating this trait have not yet been characterized. In rice, upregulation of *OsGRF4*, one of the three *VvGRF4* orthologues, leads to an increase in panicle length (Che *et al.*, 2015; Duan *et al.*, 2015), similar to the impact of mutated *VvGRF4* alleles in grapevine rachis development.

In the grapevine variety Albariño, smaller berries are associated with loose cluster architecture (Alonso-Villaverde *et al.*, 2008). In contrast, the 'Pinot noir' LCCs studied here showed an increased berry volume correlating with loose cluster architecture, which is counterintuitive at first glance. Conversely, enhanced expression of several GRFs resulted in bigger tomato fruits (Cao *et al.*, 2016), comparable to the larger berries in the 'Pinot noir' LCCs. In the same transgenic tomato plants, pedicel length increased, giving rise to a looser cyme architecture. These results suggest that GRFs are playing a role in both processes, fruit and pedicel development, of which the increase in pedicel length is the factor that has a dominating impact on grapevine cluster architecture. In the future, it will be interesting to characterize the function of individual SlGRFs in fruit and pedicel development. Specific mutations in individual *SlGRFs* introduced by CRISPR-Cas9 technology (Belhaj *et al.*, 2013) or overexpression of selected *SlGRFs* will help to understand the role of individual VvGRFs in these developmental processes.

Comparison of SEM micrographs suggested that the increase in pedicel length in LCCs is due to an enhanced number of cells at the stage of pedicel maturation. The increased number of cells could be either the result of an enhanced cell division rate or an extended window of cell proliferation. This is in line with the observation that Arabidopsis plants expressing *rGRF2* developed larger leaves harbouring more cells than control plants (Rodriguez *et al.*, 2010). Furthermore, overexpression of *VvGRF4* in Arabidopsis leads to longer pedicels, supporting the view that VvGRF4 promotes pedicel development.

VvGRF4 upregulation in LCCs is caused by mutations in the miR396 binding site

The SNP identified in M171 leads to an amino acid exchange from serine to leucine, whereas the *VvGRF4-m171-2* mutation in LCC 1-86 does not. However, both LCCs show similar inflorescence phenotypes indicating that the hindered miR396 regulation of *VvGRF4* transcript accumulation, but not the amino acid exchange, causes loose cluster architecture. Similarly, transgenic Arabidopsis plants, overexpressing the mutated versions of

© 2019 The Authors.

VvGRF4, had longer pedicels, independently of the SNP. In rice, it has been demonstrated that a 2 bp substitution in the miR396 binding site of *OsGRF4* resulting in an amino acid exchange from serine to lysine causes a similar increase in grain size as a miR396-resistant version that does not change an amino acid (Che *et al.*, 2015).

Both SNPs in M171 and 1-86 LCCs are in heterozygous condition, as expected for vegetatively propagated grapevine clones. This heterozygosity may explain the rather weak loose cluster phenotype (Figure 1), which nevertheless has a strong impact on the phytosanitary status of grapes. We speculate that a homozygous mutation would have more severe negative consequences, as exemplified by the extreme silique defects observed in homozygous OEVvGRF4-m1 and OEVvGRF4-m2 Arabidopsis plants, and would probably be unsuitable for agricultural purposes.

How can our findings be used to better understand and to modulate grapevine bunch architecture? Loose cluster architecture is associated with a large variety of phenotypic features, like smaller berries, increased rachis length, increased pedicel length, etc. We have focused on PN LCCs that develop larger berries in conjunction with longer pedicels. In all M-type and Gm-type LCC tested, we consistently found the same mutations as in M171 and in 1-86, supporting the hypothesis that these mutations are causal for the loose cluster phenotype. This raised the question, whether modulating *VvGRF4* expression is a preferred route to create loose cluster architecture. Grimplet *et al.* (2017) studied loose and compact cluster clones in the cultivar 'Garnacha Tinta', which differed in final berry number and berry size. In this case, gene expression profiling at bud burst and at the end of flowering did not reveal a differential expression of *VvGRF4*. In addition, sequencing of 13 additional loose cluster cultivars and clones did not uncover any mutation in the miR396 binding domain of *VvGRF4*. As these clones were not phenotypically characterized, we do not know, whether they show the same or different phenotypic features, in comparison with the PN clones studied. Taken together, these results indicate that probably mutations in different genes, affecting different aspects of bunch architecture, can lead to a loose cluster phenotype. In this context, *VvGRF4* homologues, which are known to be redundantly expressed in grapevine buds (Fasoli *et al.*, 2012), or other genes of the same pathway are interesting candidates. To introduce the loose cluster phenotype into other grapevine cultivars, the characterized PN alleles can be used in crosses and the identified SNPs can speed-up the breeding process by marker-assisted selection. A more advanced alternative would be to modify *VvGRF4* transcript accumulation in compact cluster varieties using CRISPR-Cas9 (Belhaj *et al.*, 2013) technology.

EXPERIMENTAL PROCEDURES

Plant material

Plant material of field grown *Vitis vinifera* ssp. vinifera (grapevine), used in this study for phenotyping and genotyping, is listed in Table S3. 'Pinot noir' (PN) clones WE M171 (M171), 1-86 Gm (1-86), Frank Charisma (FCh) and Frank Classic (FCl), used for RNA extraction, were grafted on the same root stock 125AA. *Solanum lycopersicum* (tomato) seeds of Micro-Tom wild-type and transgenic plants (lines #3 and #4), overexpressing STTM396a/396a-88, were kindly provided by Cao *et al.* (2016). Plants were grown under standard glasshouse conditions with additional artificial light (16-h photoperiod) when needed. Transgenic *Arabidopsis thaliana* (Arabidopsis) lines were in Col-0 (N1092) background. Col-0 seeds were obtained from the Nottingham Arabidopsis Stock Centre. Plants were cultivated under long day (16-h/8-h photoperiod) conditions in the greenhouse.

Morphological analyses

In total, 10 bunches per PN clone were harvested at a phenological stage of BBCH85 (Lorenz *et al.*, 1995) during the growing seasons 2015 and 2016. Bunch samples were harvested from the first bunch of shoots positioned in the centre of the fruit cane (May, 2004). After bunch destemming, single berry volume was evaluated using the image analysis software BAT (Kicherer *et al.*, 2013). The destemmed rachis was used to measure pedicel length and the distance from the node of the first lateral branch to the tip of the rachis using ImageJ software (Schneider *et al.*, 2012). Arabidopsis main inflorescence length was measured after flowering from the topmost rosette leaf to the tip of the inflorescence. Arabidopsis pedicel length was measured, when developmental stage 17 of flower development was reached (Smyth *et al.*, 1990). In tomato, measurements of pedicel length were performed, when fruits showed typical fully ripe colour. If not stated differently, detached pedicels were photographed and pedicel length was measured using ImageJ software.

Cloning and transformation

OEVvGRF4-m1, OEVvGRF4-m2 and OEVvGRF4 constructs are based on the GreenGate cloning system (Lampropoulos *et al.*, 2013) using the following modules: pGGA006 (UBI (UBIQUITIN10) promoter), pGGB003 (B-dummy), pGGD002 (D-dummy), pGGE009 (UBQ10 terminator). The resistance cassette pGGF-FAST (fluorescence-accumulating seed technology), which was introduced into pGGF000, is a modified OLE1:OLE1-RFP sequence (Shimada *et al.*, 2010) containing a 1 bp substitution in the promoter region (G688A) and three synonymous mutations in the coding sequences (CDS) (A1427G, C1454T, A1457G), to remove additional *Bsa*I sites. CDS modules of *VvGRF4-m1*, *VvGRF4-m2* and *VvGRF4* were amplified from M171, 1-86 and FCh cDNAs using Phusion Polymerase with primers XY96 and XY97 and ligated into the entry vector pGGC000. *Bsa*I restriction sites within *VvGRF4* CDS were removed by introducing the non-synonymous substitutions C669G and C941A. All modules were checked by sequencing and assembled in the destination vector pAGM4723 [a gift from Sylvestre Marillonnet; Addgene plasmid # 48015 (Weber *et al.*, 2011)], which was modified for the GreenGate cloning system. Arabidopsis Col-0 was transformed using the floral dip method (Clough and Bent, 1998) using the *A. tumefaciens* strain GV3101 (Koncz and Schell, 1986). Fluorescent seeds of T0 plants were selected. T1 plants were tested by PCR for presence of the transgene using the primers SA01 and XY98. Single copy lines were selected by

© 2019 The Authors.

qPCR, comparing the copy number of *VvGRF* to the single copy *LAS* gene. All primers are listed in Table S4.

Scanning electron microscopy

SEM was performed on a DSM 940 (Zeiss, Oberkochen, Germany) electron microscope using freeze-dried tissue. Plant material was fixed overnight in 4% glutaraldehyde solution followed by a dehydration series with up to 100% ethanol. Grapevine pedicels were additionally treated with chloroform and silica sand to remove the cuticula. All samples were critical point dried and palladium coated.

DNA analysis

Young leaves were harvested for DNA extraction, which was performed using the peqGOLD Plant DNA Mini Kit (Peqlab, Radnor, PA, USA). Construction of TruSeq DNA (PCR-free) libraries and sequencing of 2 × 100 bp paired-end read was performed at the Genome Centre of the MPIPZ, Cologne, using the Illumina HiSeq 2500 or HiSeq 3000 technology.

Read alignment against the grapevine reference sequence (Vitis_vinifera.IGGP_12x.23; ftp://ftp.ensemblgenomes.org/pub/release-23/plants/genbank/vitis_vinifera/) and variant calling were performed using bowtie2 (v.2.2.2; Langmead and Salzberg, 2012), samtools (v.0.1.19-44428cd; Li *et al.*, 2009), and shore (v.0.8; Ossowski *et al.*, 2008). SNPs and InDels were called using the following criteria: minimum base coverage 6, minimum allele frequency 0.1, minimum base quality 25. Phylogenetic analysis was done using Split4tree (v.4.11.3; Huson and Bryant, 2006), based on the alignment of artificial sequences, which were constructed with high quality variant bases at 87 genomic sites. The following criteria led to 105–192 variations in four samples: minimum coverage: 15×, minimum allele frequency: 0.2, minimum base quality: 40, maximum number of *N*s (unknown base) in reads covering the position: 3, average number of mismatches in reads covering the position: 1.5. Commonly found variations in all four samples were removed, 99 sample specific ones were retained. 12 of the 99 variations occurring either in simple repeats or in reads showing low mapping quality were removed, and therefore finally 87 SNPs were kept for phylogenetic analysis. Sequence alignment was performed using Clustal Omega (v. 1.2.4; Goujon *et al.*, 2010; Sievers *et al.*, 2011).

Sanger sequencing was performed using the 3730XL Genetic Analyzer (Applied Biosystems, Waltham, MA, USA) at the Genome Centre of the MPIPZ.

RNA analysis

Total RNA was extracted using Spectrum™ Plant Total RNA Kit (Sigma Aldrich, St. Louis, MO, USA), following protocol A and on-column DNase digestion, according to the manufacturer's protocol.

RNA-seq experiments

For RNA-seq experiments, grapevine inflorescences were harvested at three different time points:

- Stage 1: Beginning of September 2014 and 2015, 150 days after bud burst, the first inflorescence of the primary bud of latent buds (LB) was dissected. Inflorescences were prepared from LBs at positions 3 to 10 along the shoot, which had outgrown from the middle part of the fruiting cane. For each replicate, 40 inflorescences from five different plants were pooled.
- Stage 2: At bud burst, the first inflorescences of BBCH9 stage buds (Lorenz *et al.*, 1995) were dissected. Three replicates were harvested in 2015. For each replicate, 3 buds from shoots of the middle part of the fruiting cane of a single plant were used.
- Stage 3: Rachis tissue (excluding flowers and most of the pedicels) was taken from inflorescences of BBCH57 stage (just before flowering). Three biological replicates were harvested in 2015.

TruSeq Library construction and sequencing of 100 bp single reads with the Illumina HiSeq2500 or HiSeq3000 was performed at the Genome Centre of the MPIPZ, Cologne. The data are available in ENA under the study accession number PRJEB30338. Reads were mapped against the reference sequence Vitis_vinifera.IGGP_12x.23 (ftp://ftp.ensemblgenomes.org/pub/release-23/plants/genbank/vitis_vinifera/) using the software CLC Genomics workbench (v.8.5.1) with the following settings: Mismatch cost = 2, Insertion cost = 3, Deletion cost = 3, Length fraction = 0.8, Similarity fraction = 0.8, Maximum number of hits for a read = 5. Numbers of mapped reads are listed in Table S1 and RPKM (reads per kilobase of exon model per million mapped reads; Mortazavi *et al.*, 2008) values were calculated. Genes differentially expressed between loose and CCCs were identified using Baggerley *et al.*'s test (Baggerly *et al.*, 2003) and *P*-values ≤0.05 with a minimum fold change of 1.5. To calculate RPKM values of miR396, read alignment was done using tophat (v.2.1.1; Kim *et al.*, 2013), followed by bedtools (v.2.16.2; Quinlan, 2014) for read counting.

5RACE

In grapevine (Frank Charisma) and in Arabidopsis OEVvGRF4 lines #2 and #3, miR396 cleavage products of *VvGRF4* were analyzed by 5′RNA ligase-mediated rapid amplification of cDNA ends (RLM). About 5 μg total RNA, extracted from stage 3 tissue (grapevine), as well as Arabidopsis tissue including pedicels and unopened flowers, was ligated to the RNA Oligo using the GeneRacer Kit (Life Technologies, Carlsbad, CA, USA). RNA was reverse transcribed using the GeneRacer oligo(dT) primer and SuperScript III reverse transcriptase. First round and nested PCR analysis was performed using KOD polymerase and a universal forward primer together with gene-specific reverse primers. Nested PCR products were cloned into pCRII-Blunt-TOPO (Life Technologies) and 15 independent clones were sequenced by Sanger sequencing (Genome Centre, MPIPZ, Cologne) using an extended universal primer. All primers are listed in Table S4.

RT-qPCR

In grapevine, RNA was extracted from stage 2 and stage 3 tissue (as indicated above), harvested in 2015. In Arabidopsis, expression analysis was done with tissue including pedicels and unopened flowers. Next, 1 μg of total RNA was used for first-strand cDNA synthesis with oligo(dT) primer and SuperScriptIII (Fermentas) in grapevine or revertAid H Minus M-MuLV reverse transcriptase (Fermentas) in Arabidopsis. qPCRs were performed using the PowerSYBR-Green PCR Master Mix (Applied Biosystems). PCR efficiencies of the target and endogenous controls were initially validated by relative standard curves. *GAPDH* (grapevine) and *PP2A* (Arabidopsis) were used as reference genes. Relative quantification was done using the Comparative C_T Method ($\Delta\Delta C_T$). All primers are listed in Table S4. Quantification of *VvmiR396* expression was performed with the same VvRNA as indicated above and qRT-PCR was carried out according to Pantaleo *et al.* (2016) using *U6* and *5.8S* as reference genes.

ACKNOWLEDGEMENTS

The authors thank Alexandra Kalde, Ursula Pfordt, Sarina Elser and Claudia Welsch for excellent technical assistance. We thank

© 2019 The Authors.

Hernán López and Mohammad Aman Mulki for critical reading of the manuscript. The authors thank Benzhong Zhu (College of Food Science and Nutritional Engineering, China Agricultural University, Beijing, China) for seeds of the transgenic tomato lines #3 and #4, overexpressing STTM396a/396a-88. Research in the group of Eva Zyprian was supported by the Bundesministerium für Ernährung und Landwirtschaft through the grant 'Molekulare Analyse der Traubenarchitektur'. Research in the Theres laboratory was co-supported by the Bundesministerium für Ernährung und Landwirtschaft through the grant 'Molekulare Analyse der Traubenarchitektur' and by the Max Planck Society.

CONFLICT OF INTEREST

The authors declare no conflict of interest.

AUTHOR CONTRIBUTIONS

SR, RR, RT, EZ, and KT designed the research; SR, RR, performed research; SR, RR, HS, KS, EZ and KT analyzed data; SR, RR, EZ and KT wrote the manuscript.

DATA AVAILABILITY STATEMENT

Data obtained from the DNA-seq and RNA-seq have been submitted to the EMBL/GenBank database under the accession numbers PRJEB30551 and PRJEB30338, respectively. Addresses are as follows: EMBL Nucleotide Sequence Submissions: http://www.ebi.ac.uk; GenBank: http://www.ncbi.nlm.nih.gov.

SUPPORTING INFORMATION

Additional Supporting Information may be found in the online version of this article.

Figure S1. Analysis of berry size in PN clones.

Figure S2. Protein alignment of the highly conserved WRC domain of grapevine, tomato, Arabidopsis and rice growth-regulating factors (GRFs).

Figure S3. Sequence alignment of miR396 binding sites in different growth-regulating factors (GRFs) of grapevine, tomato, Arabidopsis and rice.

Figure S4. Phylogenetic tree of VvGRF4 homologues in *Vitis vinifera* (grapevine), *Arabidopsis thaliana* (Arabidopsis), *Solanum lycopersicum* (tomato) and *Oryza sativa* (rice).

Figure S5. *VvGRF4* is cleaved by miR396 in Arabidopsis.

Figure S6. *VvGRF4* overexpression plants develop more leaves and bolt later than control plants.

Figure S7. Overexpression of the mutated versions of *VvGRF4* in Arabidopsis compromises main inflorescence development and causes abnormal silique development.

Table S1. Number of mapped reads per library.

Table S2. Allele frequencies (%) of the *VvGRF4* gene in M171 and 1-86 LCCs compared with CCC derived from RNA-seq data.

Table S3. Description of phenotypes and genotypes of different grapevine cultivars.

Table S4. Primers used in this study.

Data S1. Differentially expressed genes in M171.

Data S2. Differentially expressed genes in 1-86.

Data S3. Variant details.

Data S4. Differentially expressed genes with variants.

REFERENCES

Alonso-Villaverde, V., Boso, S., Luis Santiago, J., Gago, P. and Martínez, M.-C. (2008) Relationship between susceptibility to botrytis bunch rot and grape cluster morphology in the *Vitis vinifera* L. Cultivar Albariño. *Int. J. Fruit Sci.* **8**, 251–265.

Baggerly, K.A., Deng, L., Morris, J.S. and Aldaz, C.M. (2003) Differential expression in SAGE: accounting for normal between-library variation. *Bioinformatics*, **19**, 1477–1483.

Baucher, M., Moussawi, J., Vandeputte, O.M., Monteyne, D., Mol, A., Pérez-Morga, D. and El Jaziri, M. (2013) A role for the miR396/GRF network in specification of organ type during flower development, as supported by ectopic expression of *Populus trichocarpa miR396c* in transgenic tobacco. *Plant Biol.* **15**, 892–898.

Bazin, J., Khan, G.A., Combier, J.-P. *et al.* (2013) miR396 affects mycorrhization and root meristem activity in the legume *Medicago truncatula*. *Plant J.* **74**, 920–934.

Belhaj, K., Chaparro-Garcia, A., Kamoun, S. and Nekrasov, V. (2013) Plant genome editing made easy: targeted mutagenesis in model and crop plants using the CRISPR/Cas system. *Plant Methods*, **9**, 39.

Broome, J.C., English, J.T., Marois, J.J., Latorre, B.A. and Aviles, J.C. (1995) Development of an infection model for Botrytis bunch rot of grapes based on wetness duration and temperature. *Phytopathology*, **85**, 97–102.

Cao, D., Wang, J., Ju, Z., Liu, Q., Li, S., Tian, H., Fu, D., Zhu, H., Luo, Y. and Zhu, B. (2016) Regulations on growth and development in tomato cotyledon, flower and fruit via destruction of miR396 with short tandem target mimic. *Plant Sci.* **247**, 1–12.

Carmona, M.J., Cubas, P. and Martínez-Zapater, J.M. (2002) *VFL*, the grapevine *FLORICAULA/LEAFY* ortholog, is expressed in meristematic regions independently of their fate. *Plant Physiol.* **130**, 68–77.

Che, R., Tong, H., Shi, B. *et al.* (2015) Control of grain size and rice yield by GL2-mediated brassinosteroid responses. *Nat. Plants*, **2**, 15195.

Choi, D., Kim, J.H. and Kende, H. (2004) Whole genome analysis of the *OsGRF* gene family encoding plant-specific putative transcription activators in rice (*Oryza sativa* L.). *Plant Cell Physiol.* **45**, 897–904.

Christodoulou, A.J., Weaver, R.J. and Pool, R.M. (1968) Relation of gibberellin treatment to fruit-set, berry development, and cluster compactness in *Vitis vinifera* grapes. *Proceedings of the American Society for Horticultural Science*, **92**, 301–310.

Clough, S.J. and Bent, A.F. (1998) Floral dip: a simplified method for *Agrobacterium*-mediated transformation of *Arabidopsis thaliana*. *Plant J.* 735–743.

Debernardi, J.M., Mecchia, M.A., Vercruyssen, L., Smaczniak, C., Kaufmann, K., Inze, D., Rodriguez, R.E. and Palatnik, J.F. (2014) Post-transcriptional control of *GRF* transcription factors by microRNA miR396 and GIF co-activator affects leaf size and longevity. *Plant J.* **79**, 413–426.

Deytieux-Belleau, C., Geny, L., Roudet, J., Mayet, V., Donèche, B. and Fermaud, M. (2009) Grape berry skin features related to ontogenic resistance to *Botrytis cinerea*. *Eur. J. Plant Pathol.* **125**, 551.

OIV. (2017) OIV Statistical Report on World Vitiviniculture. In *World Vitiviniculture Situation*. Paris, France: Organization Internationale de la Vigne et du Vin. http://www.oiv.int/.

Duan, P., Ni, S., Wang, J., Zhang, B., Xu, R., Wang, Y., Chen, H., Zhu, X. and Li, Y. (2015) Regulation of *OsGRF4* by OsmiR396 controls grain size and yield in rice. *Nat. Plants*, **2**, 15203.

Fasoli, M., Dal Santo, S., Zenoni, S. *et al.* (2012) The Grapevine expression atlas reveals a deep transcriptome shift driving the entire plant into a maturation program. *Plant Cell*, **24**, 3489.

Frank, R. (2006) *Im Mittelpunkt die Rebe*, 1st edn. Norderstedt, Germany: Books on Demand GmbH.

Gabler, F.M., Smilanick, J.L., Mansour, M., Ramming, D.W. and Mackey, B.E. (2003) Correlations of morphological, anatomical, and chemical features of grape berries with resistance to *Botrytis cinerea*. *Phytopathology*, **93**, 1263–1273.

Goujon, M., McWilliam, H., Li, W., Valentin, F., Squizzato, S., Paern, J. and Lopez, R. (2010) A new bioinformatics analysis tools framework at EMBL-EBI. *Nucleic Acids Res.* **38**, W695–W699.

Grimplet, J., Tello, J., Laguna, N. and Ibáñez, J. (2017) Differences in flower transcriptome between grapevine clones are related to their cluster compactness, fruitfulness, and berry size. *Front. Plant Sci.* **8**, 632–632.

© 2019 The Authors.

Hed, B., Ngugi, H.K. and Travis, J.W. (2009) Relationship between cluster compactness and bunch rot in vignoles grapes. *Plant Dis.* **93**, 1195–1201.

Hed, B., Ngugi, H.K. and Travis, J.W. (2010) Use of gibberellic acid for management of bunch rot on chardonnay and vignoles grape. *Plant Dis.* **95**, 269–278.

Hewezi, T., Maier, T.R., Nettleton, D. and Baum, T.J. (2012) The Arabidopsis microRNA396-*GRF1*/*GRF3* regulatory module acts as a developmental regulator in the reprogramming of root cells during cyst nematode infection. *Plant Physiol.* **159**, 321–335.

Horiguchi, G., Kim, G.-T. and Tsukaya, H. (2005) The transcription factor AtGRF5 and the transcription coactivator AN3 regulate cell proliferation in leaf primordia of *Arabidopsis thaliana*. *Plant J.* **43**, 68–78.

Houel, C., Martin-Magniette, M.L., Nicolas, S.D. *et al.* (2013) Genetic variability of berry size in the grapevine (*Vitis vinifera* L.). *Aust. J. Grape Wine Res.* **19**, 208–220.

Huber, H. (1965) 'Clevner Mariafeld' eine neue Blauburgunder-(Pinot noir) Selektion. *Schweizerische Zeitschrift für Obst- und Weinbau*, **101**, 160–164.

Huson, D. and Bryant, D. (2006) Application of phylogenetic networks in evolutionary studies. *Mol. Biol. Evol.* **23**, 254–267.

Kicherer, A., Roscher, R., Herzog, K., Šimon, S., Förstner, W. and Töpfer, R. (2013) BAT (Berry Analysis Tool): A high-throughput image interpretation tool to acquire the number, diameter, and volume of grapevine berries. *J. Grapevine Res.* **52**, 129–135.

Kim, J.H. and Kende, H. (2004) A transcriptional coactivator, AtGIF1, is involved in regulating leaf growth and morphology in *Arabidopsis*. *Proc. Natl Acad. Sci. USA*, **101**, 13374.

Kim, J.H. and Tsukaya, H. (2015) Regulation of plant growth and development by the GROWTH-REGULATING FACTOR and GRF-INTERACTING FACTOR duo. *J. Exp. Bot.* **66**, 6093–6107.

Kim, J.H., Choi, D. and Kende, H. (2003) The AtGRF family of putative transcription factors is involved in leaf and cotyledon growth in *Arabidopsis*. *Plant J.* **36**, 94–104.

Kim, D., Pertea, G., Trapnell, C., Pimentel, H., Kelley, R. and Salzberg, S.L. (2013) TopHat2: accurate alignment of transcriptomes in the presence of insertions, deletions and gene fusions. *Genome Biol.* **14**, R36.

van der Knaap, E., Kim, J.H. and Kende, H. (2000) A novel gibberellin-induced gene from rice and its potential regulatory role in stem growth. *Plant Physiol.* **122**, 695–704.

Koncz, C. and Schell, J. (1986) The promoter of T_L-DNA gene *5* controls the tissue-specific expression of chimaeric genes carried by a novel type of *Agrobacterium* binary vector. *Mol. General Genet.* **204**, 383–396.

Konrad, H., Lindner, B., Bleser, E. and Rühl, E.H. (2003) Strategies in the genetic selection of clones and the preservation of genetic diversity within varieties. *Acta Hortic.* **603**, 105–110.

Kuijt, S.J.H., Greco, R., Agalou, A. *et al.* (2014) Interaction between the GRF and KNOX families of transcription factors. *Plant Physiol.* **164**, 1952–1966.

Lampropoulos, A., Sutikovic, Z., Wenzl, C., Maegele, I., Lohmann, J.U. and Forner, J. (2013) GreenGate - a novel, versatile, and efficient cloning system for plant transgenesis. *PLoS ONE*, **8**, e83043.

Langmead, B. and Salzberg, S.L. (2012) Fast gapped-read alignment with Bowtie 2. *Nat. Methods*, **9**, 357.

Li, H., Handsaker, B., Wysoker, A., Fennell, T., Ruan, J., Homer, N., Marth, G., Abecasis, G., Durbin, R. and **1000 Genome Project Data Processing Subgroup**. (2009) The sequence Alignment/Map format and SAMtools. *Bioinformatics (Oxford, England)*, **25**, 2078–2079.

Liang, G., He, H., Li, Y., Wang, F. and Yu, D. (2014) Molecular mechanism of microRNA396 mediating pistil development in Arabidopsis. *Plant Physiol.* **164**, 249.

Liu, D., Song, Y., Chen, Z. and Yu, D. (2009) Ectopic expression of miR396 suppresses *GRF* target gene expression and alters leaf growth in *Arabidopsis*. *Physiol. Plant*, **136**, 223–236.

Liu, J., Hua, W., Yang, H.-L., Zhan, G.-M., Li, R.-J., Deng, L.-B., Wang, X.-F., Liu, G.-H. and Wang, H.-Z. (2012) The *BnGRF2* gene (*GRF2-like* gene from *Brassica napus*) enhances seed oil production through regulating cell number and plant photosynthesis. *J. Exp. Bot.* **63**, 3727–3740.

Liu, H., Guo, S., Xu, Y., Li, C., Zhang, Z., Zhang, D., Xu, S., Zhang, C. and Chong, K. (2014a) OsmiR396d-regulated OsGRFs function in floral organogenesis in rice through binding to their targets *OsJMJ706* and *OsCR4*. *Plant Physiol.* **165**, 160–174.

Liu, J., Rice, J.H., Chen, N., Baum, T.J. and Hewezi, T. (2014b) Synchronization of developmental processes and defense signaling by growth regulating transcription factors. *PLoS ONE*, **9**, e98477.

Lorenz, D.H., Eichhorn, K.W., Bleiholder, H., Klose, R., Meier, U. and Weber, E. (1995) Growth stages of the grapevine: phenological growth stages of the grapevine (*Vitis vinifera* L. ssp. *vinifera*)—Codes and descriptions according to the extended BBCH scale. *Aust. J. Grape Wine Res.* **1**, 100–103.

Lynn, C.D. and Jensen, F.L. (1966) Thinning effects of bloomtime gibberellin sprays on Thompson Seedless table grapes. *Am. J. Enol. Vitic.* **17**, 283.

May, P. (2004) *Flowering and Fruitset in Grapevines*. Adelaide: Lythrum Press.

Molitor, D., Behr, M., Hoffmann, L. and Evers, D. (2012) Impact of grape cluster division on cluster morphology and bunch rot epidemic. *Am. J. Enol. Vitic.* **63**, 508–514.

Mortazavi, A., Williams, B.A., McCue, K., Schaeffer, L. and Wold, B. (2008) Mapping and quantifying mammalian transcriptomes by RNA-Seq. *Nat. Methods*, **5**, 621–628.

Mosesian, R.M. and Nelson, K.E. (1968) Effect on 'Thompson Seedless' fruit of gibberellic acid bloom sprays and double girdling. *Am. J. Enol. Vitic.* **19**, 37.

Nair, N.G. and Allen, R.N. (1993) Infection of grape flowers and berries by *Botrytis cinerea* as a function of time and temperature. *Mycol. Res.* **97**, 1012–1014.

Omidbakhshfard, M.A., Proost, S., Fujikura, U. and Mueller-Roeber, B. (2015) Growth-regulating factors (GRFs): a small transcription factor family with important functions in plant biology. *Mol. Plant*, **8**, 998–1010.

Omidbakhshfard, M.A., Fujikura, U., Olas, J.J., Xue, G.-P., Balazadeh, S. and Mueller-Roeber, B. (2018) GROWTH-REGULATING FACTOR 9 negatively regulates arabidopsis leaf growth by controlling *ORG3* and restricting cell proliferation in leaf primordia. *PLoS Genet.* **14**, e1007484–e1007484.

Ossowski, S., Schneeberger, K., Clark, R.M., Lanz, C., Warthmann, N. and Weigel, D. (2008) Sequencing of natural strains of *Arabidopsis thaliana* with short reads. *Genome Res.* **18**, 2024–2033.

Pajoro, A., Madrigal, P., Muiño, J.M. *et al.* (2014) Dynamics of chromatin accessibility and gene regulation by MADS-domain transcription factors in flower development. *Genome Biol.* **15**, R41.

Pantaleo, V., Vitali, M., Boccacci, P., Miozzi, L., Cuozzo, D., Chitarra, W., Mannini, F., Lovisolo, C. and Gambino, G. (2016) Novel functional microRNAs from virus-free and infected *Vitis vinifera* plants under water stress. *Sci. Rep.* **6**, 20167.

Pertot, I., Giovannini, O., Benanchi, M., Caffi, T., Rossi, V. and Mugnai, L. (2017) Combining biocontrol agents with different mechanisms of action in a strategy to control *Botrytis cinerea* on grapevine. *Crop Prot.* **97**, 85–93.

Pieri, P., Zott, K., Gomès, E. and Hilbert, G. (2016) Nested effects of berry half, berry and bunch microclimate on biochemical composition in grape. *OENO One*, **50**, 23.

Porten, M. (2001) *Die Spätburgunderklone – Klontypen*. Neustadt, Germany: DLR, Fachinformationen.

Pratt, C. (1971) Reproductive anatomy in cultivated grapes - a review. *Am. J. Enol. Vitic.* **22**, 92.

Quinlan, A.R. (2014) BEDTools: the Swiss-Army tool for genome feature analysis. *Curr. Protoc. Bioinformat.* **47**, 11.12.11–11.12.34.

Rehmsmeier, M., Steffen, P., Höchsmann, M. and Giegerich, R. (2004) Fast and effective prediction of microRNA/target duplexes. *RNA*, **10**, 1507–1517.

Richter, R., Gabriel, D., Rist, F., Töpfer, R. and Zyprian, E. (2019) Identification of co-located QTLs and genomic regions affecting grapevine cluster architecture. *Theor. Appl. Genet.* **132**(4), 1159–1177.

Rodriguez, R.E., Mecchia, M.A., Debernardi, J.M., Schommer, C., Weigel, D. and Palatnik, J.F. (2010) Control of cell proliferation in *Arabidopsis thaliana* by microRNA miR396. *Development*, **137**, 103.

Sarooshi, R. (1977) Some effects of girdling, gibberellic acid sprays, bunch thinning and trimming on the sultana. *Aust. J. Exp. Agric.* **17**, 700–704.

Schmid, J., Manty, F., Lindner, B., Ries, R., Rühl, E., Konrad, H., Schönhals, E. and Bleser, E. (2009) *Geisenheimer Rebsorten und Klone*. Geisenheim: Gesellschaft zur Förderung der Forschungsanstalt Geisenheim.

Schneider, C.A., Rasband, W.S. and Eliceiri, K.W. (2012) NIH Image to ImageJ: 25 years of image analysis. *Nat. Methods*, **9**, 671–675.

© 2019 The Authors.

Shavrukov, Y.N., Dry, I.B. and Thomas, M.R. (2004) Inflorescence and bunch architecture development in *Vitis vinifera* L. *Aust. J. Grape Wine Res.* **10**, 116–124.

Shimada, T.L., Shimada, T. and Hara-Nishimura, I. (2010) A rapid and non-destructive screenable marker, FAST, for identifying transformed seeds of *Arabidopsis thaliana*. *Plant J.* **61**, 519–528.

Sievers, F., Wilm, A., Dineen, D. *et al.* (2011) Fast, scalable generation of high-quality protein multiple sequence alignments using Clustal Omega. *Mol. Syst. Biol.* **7**, 539–539.

Smyth, D.R., Bowman, J.L. and Meyerowitz, E.M. (1990) Early flower development in Arabidopsis. *Plant Cell*, **2**, 755–767.

Tello, J. and Ibáñez, J. (2017) What do we know about grapevine bunch compactness? A state-of-the-art review. *Aust. J. Grape Wine Res.* **24**, 6–23.

Tello, J., Aguirrezábal, R., Hernáiz, S., Larreina, B., Montemayor, M.I., Vaquero, E. and Ibáñez, J. (2015) Multicultivar and multivariate study of the natural variation for grapevine bunch compactness. *Aust. J. Grape Wine Res.* **21**, 277–289.

Vail, M.E. (1991) Grape cluster architecture and the susceptibility of berries to *Botrytis cinerea*, *Phytopathology*, **81**, 188–191.

Vail, M.E., Wolpert, J.A., Gubler, W.D. and Rademacher, M.R. (1998) Effect of cluster tightness on Botrytis bunch rot in six Chardonnay clones. *Plant Dis.* **82**, 107–109.

Valdés-Gómez, H., Fermaud, M., Roudet, J., Calonnec, A. and Gary, C. (2008) Grey mould incidence is reduced on grapevines with lower vegetative and reproductive growth. *Crop Prot.* **27**, 1174–1186.

Wang, L., Gu, X., Xu, D., Wang, W., Wang, H., Zeng, M., Chang, Z., Huang, H. and Cui, X. (2011) miR396-targeted AtGRF transcription factors are required for coordination of cell division and differentiation during leaf development in *Arabidopsis*. *J. Exp. Bot.* **62**, 761–773.

Wang, F., Qiu, N., Ding, Q., Li, J., Zhang, Y., Li, H. and Gao, J. (2014) Genome-wide identification and analysis of the growth-regulating factor family in Chinese cabbage (*Brassica rapa* L. ssp. *pekinensis*). *BMC Genomics*, **15**(1), 807.

Weber, E., Engler, C., Gruetzner, R., Werner, S. and Marillonnet, S. (2011) A modular cloning system for standardized assembly of multigene constructs. *PLoS ONE*, **6**, e16765–e16765.

Wu, L., Zhang, D., Xue, M., Qian, J., He, Y. and Wang, S. (2014) Overexpression of the maize *GRF10*, an endogenous truncated growth-regulating factor protein, leads to reduction in leaf size and plant height. *J. Integr. Plant Biol.* **56**, 1053–1063.

Yamaguchi, N. and Komeda, Y. (2013) The role of CORYMBOSA1/BIG and auxin in the growth of *Arabidopsis* pedicel and internode. *Plant Sci.* **209**, 64–74.

Zhang, D.-F., Li, B., Jia, G.-Q., Zhang, T.-F., Dai, J.-R., Li, J.-S. and Wang, S.-C. (2008) Isolation and characterization of genes encoding GRF transcription factors and GIF transcriptional coactivators in Maize (*Zea mays* L.). *Plant Sci.* **175**, 809–817.

© 2019 The Authors.
The Plant Journal published by Society for Experimental Biology and John Wiley & Sons Ltd,